

Generalizing Random-Vector SLAM with Random Finite Sets

Keith Y. K. Leung*, Felipe Inostroza[†], Martin Adams[‡]

Advanced Mining Technology Center (AMTC), Universidad de Chile, Santiago, Chile
keith.leung@amtc.uchile.cl*, finostro@ug.uchile.cl[†], martin@ing.uchile.cl[‡]

Abstract—The simultaneous localization and mapping (SLAM) problem in mobile robotics has traditionally been formulated using random vectors. Alternatively, random finite sets (RFSs) can be used in the formulation, which incorporates non-heuristic-based data association and detection statistics within an estimator that provides both spatial and cardinality estimates of landmarks. This paper mathematically shows that the two formulations are actually closely related, and that RFS SLAM can be viewed as a generalization of vector-based SLAM. Under a set of ideal detection conditions, the two methods are equivalent. This is validated by using simulations and real experimental data, by comparing principled realizations of the two formulations.

I. INTRODUCTION

Simultaneous localization and mapping (SLAM) is a problem in robotics in which a robot uses its available sensor measurements to estimate a map of the operating environment, while concurrently estimating its pose relative to the map. The general probabilistic approach currently adopted by the mobile robotics community uses random vectors to represent the robot and map state, and solves for SLAM solution through stochastic filtering, or batch estimation [1]. Recently, a random finite set (RFS) formulation was introduced for feature-based maps [2], where random vectors representing landmark spatial estimates are placed in a set in which the cardinality (or size) is a random variable. The map update process in RFS-based filters, such as those in [2, 3, 4, 5], may appear vastly different compared to vector-based approaches. However, there is actually a close relationship between the two SLAM formulations. The objective of this paper is to uncover this relationship, and show the conditions under which RFS SLAM reduces to random-vector SLAM. Furthermore, it explains why random vector formulations tend to fail in high-clutter conditions while RFS SLAM is able to operate robustly.

Similar to vector-based filtering methods such as the Kalman filter (KF), RFS-based filtering methods also stem from the the recursive Bayesian filtering paradigm. A set of mathematical tools called finite set statistics (FISST) was developed by Mahler [6], which include the definitions for set integrals and derivatives, and allows the application of Bayes estimation techniques for use with RFSs. Aside from the benefit of estimating the number of landmarks that have entered the robot’s field of view (FOV), RFS SLAM does not require heuristic-based data association (i.e., determining the correspondences between landmarks and measurements), and is able to incorporate detection statistics (i.e., probabilities of detection and clutter intensity) within the estimator. This paper will show that given the restrictive conditions of having

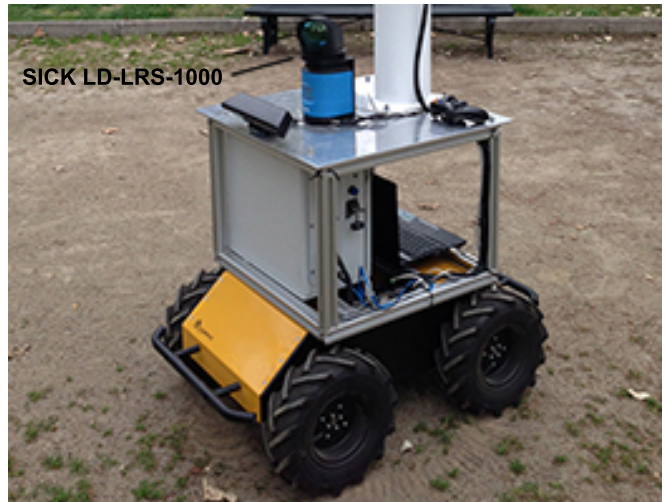


Fig. 1: The Clearpath Husky A200 robot used for dataset collection. It was equipped with a SICK LD-LRS-1000 lidar.

a deterministic map size, perfect detection probabilities, and the absence of false measurements, RFS SLAM reduces to a random-vector SLAM formulation. The paper is organized as follows: The vector-based and RFS-based SLAM formulations will first be presented in Section II. Section III will show how RFS SLAM is a generalization of vector-based SLAM. This claim is validated in Section IV using simulations and real experimental data collected using the robot shown in Fig. 1.

II. SLAM FORMULATION

SLAM is a state estimation problem in which the goal is to calculate an estimate of the robot trajectory and map feature positions over time by using all available sensor measurements. In general, the underlying stochastic system of the mobile robot and its sensors can be represented using the non-linear discrete-time equations:

$$\mathbf{x}_k = \mathbf{g}(\mathbf{x}_{k-1}, \mathbf{u}_k, \boldsymbol{\delta}_k) \quad (1)$$

$$\mathbf{z}_k^j = \mathbf{h}(\mathbf{x}_k, \mathbf{m}^i, \boldsymbol{\epsilon}_k) \quad (2)$$

where

\mathbf{x}_k represents the robot pose at time-step k ,

\mathbf{g} is the robot motion model,

\mathbf{u}_k is the the odometry measurement at time-step k ,

$\boldsymbol{\delta}_k$ is the process noise at time-step k ,

\mathbf{z}_k^j is the j -th measurement vector at time-step k

\mathbf{h} is the sensor-specific measurement model,

\mathbf{m}^i is a random vector for the position of landmark i ,

ϵ_k is the measurement noise

The set of all n measurements at time-step k is defined as:

$$\mathcal{Z}_k \equiv \{\mathbf{z}_k^1, \mathbf{z}_k^2, \dots, \mathbf{z}_k^n\} \quad (3)$$

The random vectors representing observed landmarks can be concatenated into a single random vector:

$$\mathbf{m} = (\mathbf{m}^1, \mathbf{m}^2, \dots, \mathbf{m}^m) \quad (4)$$

In the current vector-based formulation, the goal is to calculate the posterior:

$$p(\mathbf{x}_{0:k}, \mathbf{m} | \mathcal{Z}_{1:k}, \mathbf{u}_{0:k}) \quad (5)$$

Using a probabilistic framework and a filtering approach, this can be calculated recursively by Bayesian estimation:

$$\begin{aligned} & p(\mathbf{x}_{0:k}, \mathbf{m} | \mathcal{Z}_{1:k-1}, \mathbf{u}_{0:k}) \\ &= p(\mathbf{x}_k | \mathbf{x}_{k-1}, \mathbf{u}_k) p(\mathbf{x}_{0:k-1}, \mathbf{m} | \mathcal{Z}_{1:k-1}, \mathbf{u}_{0:k-1}) \end{aligned} \quad (6)$$

$$\begin{aligned} & p(\mathbf{x}_{0:k}, \mathbf{m} | \mathcal{Z}_{1:k}, \mathbf{u}_{0:k}) \\ &= \frac{p(\mathcal{Z}_k | \mathbf{x}_{0:k}, \mathbf{m}) p(\mathbf{x}_{0:k}, \mathbf{m} | \mathcal{Z}_{1:k-1}, \mathbf{u}_{0:k})}{\int p(\mathcal{Z}_k | \mathbf{x}_{0:k}, \mathbf{m}) p(\mathbf{m} | \mathcal{Z}_{1:k-1}, \mathbf{x}_{0:k}) d\mathbf{m}} \end{aligned} \quad (7)$$

Alternatively, the SLAM formulation can be generalized by placing map vectors into a RFS:

$$\mathcal{M}_k \equiv \{\mathbf{m}^1, \mathbf{m}^2, \dots, \mathbf{m}^m\}, \quad (8)$$

where the number of landmarks, $|\mathcal{M}_k| = m$, is also a random variable. From this, (5) can be rewritten as

$$p(\mathbf{x}_{0:k}, \mathcal{M}_k | \mathcal{Z}_{1:k}, \mathbf{u}_{0:k}), \quad (9)$$

and can also theoretically be solved by Bayesian estimation:

$$\begin{aligned} & p(\mathbf{x}_{0:k}, \mathcal{M}_k | \mathcal{Z}_{1:k-1}, \mathbf{u}_{0:k}) \\ &= p(\mathbf{x}_k | \mathbf{x}_{k-1}, \mathbf{u}_k) p(\mathbf{x}_{0:k-1}, \mathcal{M}_{k-1} | \mathcal{Z}_{1:k-1}, \mathbf{u}_{0:k-1}) \end{aligned} \quad (10)$$

$$\begin{aligned} & p(\mathbf{x}_{0:k}, \mathcal{M}_k | \mathcal{Z}_{1:k}, \mathbf{u}_{0:k}) \\ &= \frac{p(\mathcal{Z}_k | \mathbf{x}_{0:k}, \mathcal{M}_k) p(\mathbf{x}_{0:k}, \mathcal{M}_k | \mathcal{Z}_{1:k-1}, \mathbf{u}_{0:k})}{\int p(\mathcal{Z}_k | \mathbf{x}_{0:k}, \mathcal{M}_k) p(\mathcal{M}_k | \mathcal{Z}_{1:k-1}, \mathbf{x}_{0:k}) d\mathcal{M}_k} \end{aligned} \quad (11)$$

The relationship between the RFS and random vector formulations will be revealed next.

III. GENERALIZATION OF VECTOR-BASED SLAM

Vector-based SLAM generally requires methods for data association and map management routines that determine the dimension of \mathbf{m} . In contrast, the number of landmarks is estimated as part of the RFS SLAM formulation. Additionally, detection and clutter statistics are accounted for. Hence, RFS-SLAM can be viewed as a generalization of vector-based SLAM. To support this claim, it is necessary to show the conditions under which (11) reduces to (7). Therefore, the three critical factors in (11) will be examined: a) The joint distribution for the robot trajectory and the map, $p(\mathbf{x}_{0:k}, \mathcal{M}_k | \mathcal{Z}_{1:k-1}, \mathbf{u}_{0:k})$, b) the measurement likelihood, $p(\mathcal{Z}_k | \mathbf{x}_{0:k}, \mathbf{m})$, and c) the normalizing factor.

A. The Joint Distribution for Robot Trajectory and Map

Using FISST [6], the distribution over the robot trajectory and map can be factored as:

$$\begin{aligned} & p(\mathbf{x}_{0:k}, \mathcal{M}_k | \mathcal{Z}_{1:k-1}, \mathbf{u}_{0:k}) \\ &= p(\mathcal{M}_k | \mathbf{x}_{0:k}, \mathcal{Z}_{1:k-1}, \mathbf{u}_{0:k}) p(\mathbf{x}_{0:k} | \mathcal{Z}_{1:k-1}, \mathbf{u}_{0:k}) \\ &= m! p_{|\mathcal{M}_k|}(m) p(\mathbf{m}^1 | \mathbf{x}_{0:k}, \mathcal{Z}_{1:k-1}, \mathbf{u}_{0:k}) \times \\ & \quad p(\mathbf{m}^2 | \mathbf{x}_{0:k}, \mathcal{Z}_{1:k-1}, \mathbf{u}_{0:k}) \times \dots \times \\ & \quad p(\mathbf{m}^m | \mathbf{x}_{0:k}, \mathcal{Z}_{1:k-1}, \mathbf{u}_{0:k}) p(\mathbf{x}_{0:k} | \mathcal{Z}_{1:k-1}, \mathbf{u}_{0:k}) \end{aligned} \quad (12)$$

where $m!$ represents all the different permutations of the members in \mathcal{M}_k . The probability mass function (PMF) $p_{|\mathcal{M}_k|}(m)$ is the likelihood of \mathcal{M}_k having a cardinality of m . In a vector-based approach, the number of landmarks is not treated as a random variable in the map estimator, and is often fixed by an external map management routine (i.e., $p_{|\mathcal{M}_k|}(m) = 1$). Furthermore, vector-based approaches select one landmark ordering out of all permutations (i.e., $1/m!$). Applying these:

$$\begin{aligned} & \frac{1}{m!} p(\mathbf{x}_{0:k}, \mathcal{M}_k | \mathcal{Z}_{1:k-1}, \mathbf{u}_{0:k}), \quad p_{|\mathcal{M}_k|}(m) = 1 \\ &= p(\mathbf{m}^1 | \mathbf{x}_{0:k}, \mathcal{Z}_{1:k-1}, \mathbf{u}_{0:k}) p(\mathbf{m}^2 | \mathbf{x}_{0:k}, \mathcal{Z}_{1:k-1}, \mathbf{u}_{0:k}) \times \dots \times \\ & \quad p(\mathbf{m}^m | \mathbf{x}_{0:k}, \mathcal{Z}_{1:k-1}, \mathbf{u}_{0:k}) p(\mathbf{x}_{0:k} | \mathcal{Z}_{1:k-1}, \mathbf{u}_{0:k}) \\ &= p(\mathbf{m} | \mathbf{x}_{0:k}, \mathcal{Z}_{1:k-1}, \mathbf{u}_{0:k}) p(\mathbf{x}_{0:k} | \mathcal{Z}_{1:k-1}, \mathbf{u}_{0:k}) \\ &= p(\mathbf{x}_{0:k}, \mathbf{m} | \mathcal{Z}_{1:k-1}, \mathbf{u}_{0:k}) \end{aligned} \quad (13)$$

This result is the same as the vector-based joint distribution for the robot trajectory and the map, in the numerator of (7).

B. Measurement Likelihood

In vector-based approaches, an outlier rejection algorithm is often used to discard false measurements. From the remaining set of true measurements, data association is performed to determine correspondences to landmark estimates. Let $\theta(i) = j$ represent the association of landmark i with measurement j . The vector-based measurement likelihood can be expressed as:

$$p(\mathcal{Z}_k | \mathbf{x}_{0:k}, \mathbf{m}) = \prod_{\substack{j=1 \\ \exists i, \theta(i)=j}}^n p(\mathbf{z}_k^j | \mathbf{m}^{\theta(j)}, \mathbf{x}_{0:k}) \quad (14)$$

For the presentation of the set measurement likelihood, let:

$$\mathcal{Z}_k^0 \equiv \mathcal{Z}_k \quad (15)$$

$$\mathcal{Z}_k^1 \equiv \{\mathcal{Z}_k^0 - \{\mathbf{z}^1\}\}, \quad \mathbf{z}^1 \in \mathcal{Z}_k^0 \quad (16)$$

$$\mathcal{Z}_k^r \equiv \{\mathcal{Z}_k^{r-1} - \{\mathbf{z}^r\}\}, \quad \mathbf{z}^r \in \mathcal{Z}_k^{r-1} \quad (17)$$

where \mathcal{Z}_k^0 is the set of measurements at time-step k . \mathcal{Z}_k^1 is the set of measurement with one measurement taken away from set \mathcal{Z}_k^0 . Continuing with this pattern, \mathcal{Z}_k^2 is the set of measurements with a measurement taken away from \mathcal{Z}_k^1 . The set measurement likelihood can then be written as (18). The first term considers all measurements as clutter, the second term considers all but one measurement as clutter, etc. These terms can be written more compactly according to the last line, where the variable r represents the number of measurement to landmark correspondences. The upper limit

$$\begin{aligned}
& p(\mathcal{Z}_k | \mathcal{M}_k, \mathbf{x}_{0:k}) = p(\mathcal{Z}_k | \{\mathbf{m}^1, \mathbf{m}^2, \dots, \mathbf{m}^m\}, \mathbf{x}_{0:k}) \\
& = p_{\kappa}(\mathcal{Z}_k) \prod_{i=1}^m (1 - P_D(\mathbf{m}^i)) + \sum_{\mathbf{y}^1 \in \mathcal{Z}_k^0} \left(p_{\kappa}(\mathcal{Z}_k^1) \prod_{i=1}^1 (P_D(\mathbf{x}_k, \mathbf{m}^i) p(\mathbf{y}^1 | \mathbf{m}^i, \mathbf{x}_{0:k})) \prod_{i=2}^m (1 - P_D(\mathbf{m}^i)) \right) + \dots + \\
& \quad \sum_{\mathbf{y}^1 \in \mathcal{Z}_k^0} \sum_{\mathbf{y}^2 \in \mathcal{Z}_k^1} \dots \sum_{\mathbf{y}^r \in \mathcal{Z}_k^{r-1}} \left(p_{\kappa}(\mathcal{Z}_k^r) \prod_{i=1}^r (P_D(\mathbf{x}_k, \mathbf{m}^i) p(\mathbf{y}^i | \mathbf{m}^i, \mathbf{x}_{0:k})) \prod_{i=r+1}^m (1 - P_D(\mathbf{m}^i)) \right) + \dots \\
& = \sum_{r=0}^{\min(m,n)} \left\{ \sum_{\mathbf{y}^1 \in \mathcal{Z}_k^0} \sum_{\mathbf{y}^2 \in \mathcal{Z}_k^1} \dots \sum_{\mathbf{y}^r \in \mathcal{Z}_k^{r-1}} \left(p_{\kappa}(\mathcal{Z}_k^r) \prod_{i=1}^r (P_D(\mathbf{x}_k, \mathbf{m}^i) p(\mathbf{y}^i | \mathbf{m}^i, \mathbf{x}_{0:k})) \prod_{i=r+1}^m (1 - P_D(\mathbf{m}^i)) \right) \right\} \quad (18)
\end{aligned}$$

of r cannot exceed the number of measurements, n , nor the number of landmark estimates, m . For a given number of pairings (i.e., a given value of r), all permutations of measurement to landmark estimate pairings are considered. Unpaired measurements give the clutter factor, $p_{\kappa}(\cdot)$. Paired couples (from $i = \{1 \dots r\}$) provide the probability of detection and the single-landmark measurement likelihood factors, $(P_D^i) p(\mathbf{z}^i | \mathbf{m}^i, \mathbf{x}_{0:k})$. Unpaired landmark estimates give the mis-detection factors, $(1 - P_D^i)$.

In vector-based SLAM, landmark estimates without an associated measurement remain unchanged by retaining their current estimate. This can be mimicked in RFS SLAM by setting the probability of detection to 1 for a measurement-associated landmark, and to 0 for non-associated ones:

$$P_D(\mathbf{x}_k, \mathbf{m}^i) = \begin{cases} 1 & \text{if } \theta(i) \neq 0 \\ 0 & \text{else} \end{cases} \quad (19)$$

Let Θ represent the number of landmarks with associated measurements. All the terms in (18) for which $r < \Theta$ will equate to 0 because there will be at least one probability of mis-detection factor in each of these terms that equals 0. Furthermore, all the terms for which $r > \Theta$ in (18) will also equate to 0 because there will be at least one probability of detection factor in each of those term that equals 0. Additionally, for the $r = \Theta$ case, terms that do not agree with the data association hypothesis will also equate to 0. As a result, under these specific conditions, the set measurement likelihood simplifies to:

$$p(\mathcal{Z}_k | \mathcal{M}_k, \mathbf{x}_{0:k}) = p_{\kappa}(\mathcal{Z}_k^{\Theta}) \prod_{\substack{j=1 \\ \exists i, \theta(i)=j}}^n p(\mathbf{z}_k^j | \mathbf{m}^{\theta(j)}, \mathbf{x}_{0:k}) \quad (20)$$

where the left-most factor treats all the non-associated measurements as clutter, while the remaining factor includes the measurement likelihoods of all the associated measurements. Since false measurements from clutter are discarded in vector-based SLAM, they should not affect the measurement likelihood. Assuming that the clutter is distributed according to an

independently and identically distributed (IID) cluster process:

$$p_{\kappa}(\mathcal{Z}_k^{\Theta}) = (|\mathcal{Z}_k| - \Theta)! p_{|\mathcal{Z}_k^{\Theta}|}(|\mathcal{Z}_k| - \Theta) \prod_{\substack{j=1 \\ \exists i, \theta(i)=j}}^n p_{\kappa}(\mathbf{z}_k^j) \quad (21)$$

If the statistics for non-associated measurements are

$$p_{\kappa}(\mathbf{z}) = \begin{cases} 1 & \text{if } \mathbf{z} \in \mathcal{Z}_k^{\Theta} \\ 0 & \text{else} \end{cases} \quad (22)$$

$$p_{|\mathcal{Z}_k^{\Theta}|}(|\mathcal{Z}_k| - \Theta) = \frac{1}{(|\mathcal{Z}_k| - \Theta)!} \quad (23)$$

(by inspection) then substituting (21) (with (22) and (23)) into (20) yields the vector-based measurement likelihood (14):

$$p(\mathcal{Z}_k | \mathcal{M}_k, \mathbf{x}_{0:k}) = \prod_{\substack{j=1 \\ \exists i, \theta(i)=j}}^n p(\mathbf{z}_k^j | \mathbf{m}^{\theta(j)}, \mathbf{x}_{0:k}), \quad (24)$$

C. The Normalization Factor

The update equation from the Bayes filter (7) in the random vector form contains a normalizing factor that can be written in the form of an integral:

$$\int p(\mathcal{Z}_k | \mathbf{x}_{0:k}, \mathbf{m}^1, \dots, \mathbf{m}^m) \times p(\mathbf{m}^1, \dots, \mathbf{m}^m | \mathcal{Z}_{1:k-1}, \mathbf{x}_{0:k}) d\mathbf{m}^1 \dots d\mathbf{m}^m \quad (25)$$

The corresponding expression to (25) in RFS form can be partially expanded according to FISST [6]:

$$\begin{aligned}
& \int p(\mathcal{Z}_k | \mathcal{M}_k, \mathbf{x}_{0:k}) p(\mathcal{M}_k | \mathbf{x}_{0:k}, \mathcal{Z}_{1:k-1}) d\mathcal{M}_k \\
& = p(\mathcal{Z}_k, \emptyset | \mathbf{x}_{0:k}, \mathcal{Z}_{1:k-1}) + \int p(\mathcal{Z}_k, \mathbf{m}^1 | \mathbf{x}_{0:k}, \mathcal{Z}_{1:k-1}) d\mathbf{m}^1 + \\
& \quad \iint p(\mathcal{Z}_k, \mathbf{m}^1, \mathbf{m}^2 | \mathbf{x}_{0:k}, \mathcal{Z}_{1:k-1}) d\mathbf{m}^1 d\mathbf{m}^2 + \dots + \\
& \quad \iint p(\mathcal{Z}_k | \mathbf{m}^1, \mathbf{m}^2, \mathbf{x}_{0:k}, \mathcal{Z}_{1:k-1}) p(\mathbf{m}^1, \mathbf{m}^2 | \mathbf{x}_{0:k}, \mathcal{Z}_{1:k-1}) \\
& \quad \quad d\mathbf{m}^1 d\mathbf{m}^2 + \dots + \\
& \quad \int \dots \int p(\mathcal{Z}_k | \mathbf{m}^1, \dots, \mathbf{m}^m, \mathbf{x}_{0:k}, \mathcal{Z}_{1:k-1}) \\
& \quad \quad p(\mathbf{m}^1, \dots, \mathbf{m}^m | \mathbf{x}_{0:k}, \mathcal{Z}_{1:k-1}) d\mathbf{m}^1 \dots d\mathbf{m}^m + \dots \quad (26)
\end{aligned}$$

The set integral is a summation series since it considers maps of every possible finite size, including an empty map. By fixing the size of the map to m (i.e., as determined by a map management process), the expression in (26) simplifies greatly, as the term corresponding with the fixed map size will be the only one that remains, and (26) then becomes (25):

$$\begin{aligned} & \int p(\mathcal{Z}_k | \mathcal{M}_k, \mathbf{x}_{0:k}) p(\mathcal{M}_k | \mathbf{x}_{0:k}, \mathcal{Z}_{1:k-1}) d\mathcal{M}_k, |\mathcal{M}_k| = m \\ = & \int \cdots \int p(\mathcal{Z}_k | \mathbf{m}^1, \dots, \mathbf{m}^m, \mathbf{x}_{0:k}, \mathcal{Z}_{1:k-1}) \\ & p(\mathbf{m}^1, \dots, \mathbf{m}^m | \mathbf{x}_{0:k}, \mathcal{Z}_{1:k-1}) d\mathbf{m}^1 \dots d\mathbf{m}^m \end{aligned} \quad (27)$$

In summary, it has been shown that the Bayes estimator in RFS representation is equivalent to the random vector representation under the following conditions, which from hereon will be referred to as the *ideal detection conditions*:

- The size of the map estimate is deterministic.
- Data association is deterministic.
- The probability of detection of a landmark with an associated measurement equals 1, and equals 0 if not associated.
- The likelihood of non-associated measurements being clutter is equal 1.

IV. EXPERIMENTS

Simulated and real outdoor experimental data were used to validate the claim that RFS SLAM is equivalent to vector-based SLAM under the ideal detection conditions. Without further assumptions, the full RFS Bayesian estimates are intractable in both the vector and set-based frameworks. Therefore, the validation will be based on principled realizations of the Bayes estimator. The Rao-Blackwellized (RB)-probability hypothesis density (PHD) SLAM algorithm as detailed in [7, 8] will be used as the RFS SLAM implementation, while the factored solution to SLAM (FastSLAM) [9] algorithm will be used as the vector-based implementation¹. Both algorithms are similar in that a RB particle filter (PF) is used in the estimate with a factored form of the SLAM posterior. In both cases, the robot trajectory is estimated with particles. RB-PHD SLAM uses Gaussian mixture (GM)-PHD filters [10] for the map update, while FastSLAM uses Extended Kalman filters (EKF) [11].

For a fair comparison, both SLAM algorithms used 200 particles. FastSLAM was implemented with a binary Bayes filter that accounted for detection statistics for the purpose of map management. Landmark estimates with a log-odds of existence below -5.0 were pruned, as part of the map management routine. For data association in FastSLAM, the Hungarian Method [12] was used to determine the set of correspondences that gave the highest combined measurement likelihood for a given set of measurements.

¹The implementation of RB-PHD SLAM and FastSLAM used can be found in the open-source C++ RFS-SLAM library at <https://github.com/kykleung/RFS-SLAM.git>.

A. Simulations

The use of simulations allowed detection statistics to be controlled. In a simulated 2-D space, the robot traversed through a landmark-populated environment while obtaining range-bearing measurements from landmarks between 5m to 25m in any direction. All landmarks were assumed to have the same probability of detection. False measurements were added according to the clutter intensity. The number of clutter measurements was assumed to be Poisson distributed, while the clutter intensity was uniformly distributed over the measurement space. Theoretically, under near perfect probabilities of detection, and low clutter intensity, RB-PHD SLAM should perform similarly to FastSLAM. When the probabilities of detection are low, and clutter intensity is high, RB-PHD SLAM should produce more consistent estimates as it accounts for the detection statistics. The following cases were tested:

- 1) High probability of detection ($P_D = 0.99$), and low clutter intensity ($\kappa = 0.000001\text{m}^{-2}$)
- 2) Low probability of detection ($P_D = 0.50$), and high clutter intensity ($\kappa = 0.005000\text{m}^{-2}$)

The expected number of false measurements per time-step is 0.0019 for case 1, and 9.45 for case 2.

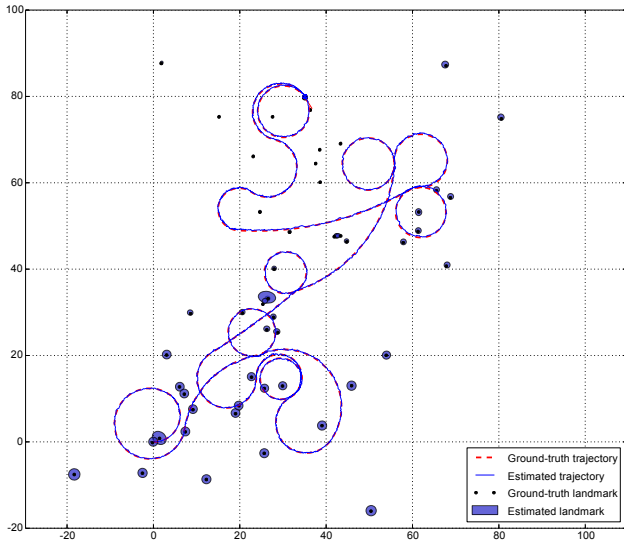
The map and trajectory estimates of both SLAM algorithms for case 1 are shown in Fig. 2. Both methods performed similarly as hypothesized.

For case 2, FastSLAM was expected to have difficulties due to the implicitly assumed ideal detection conditions inherent in vector-based SLAM. The simulated conditions made it difficult for data association to assign proper correspondences, thus causing the estimates to diverge. Fig. 3 shows the map and trajectory estimates from the two algorithms. As predicted, RB-PHD-SLAM was able to produce a consistent map, with a trajectory estimate that followed closely to the real robot trajectory. On the contrary, the FastSLAM solution diverged. High-opacity ellipses in the results have Gaussian weights or probabilities of existence close to 1.

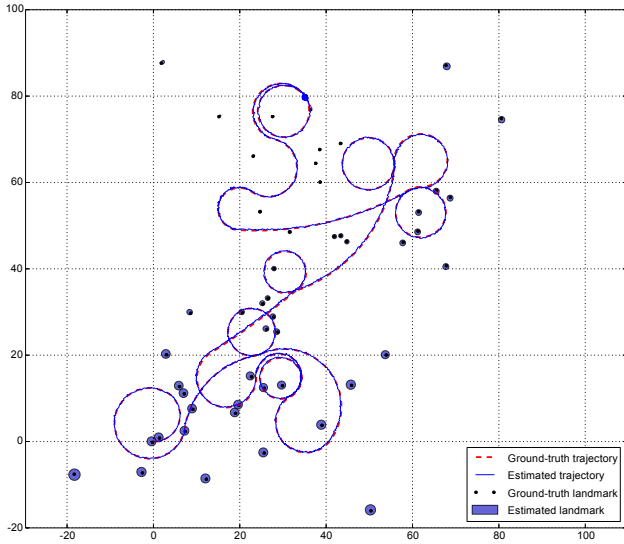
B. Outdoor Experiments

To further validate the earlier hypotheses on the performance of the two SLAM algorithms under different detection conditions, two outdoor datasets were collected in Parque O'Higgins, Santiago, Chile, using the mobile robot shown in Fig. 1. The location is a municipal park, and data collection was conducted in an area of approximately $100\text{m} \times 100\text{m}$. The two datasets were collected at different times of the day, with the first being early in the morning when the park is free of people and other moving objects such as cars. The second dataset was collected in the late morning, when there are significantly more moving people and cars.

Wheel encoders on the robot provided odometry measurements. A SICK LD-LRS-1000 scanning lidar was mounted on the robot and produced 2-D scans with a resolution of 0.5 degrees at 7 Hz. A customized detector [13] was used to extract circular-like objects. A global positioning system (GPS) receiver was also used during data collection, but the coverage



(a) RB-PHD-SLAM

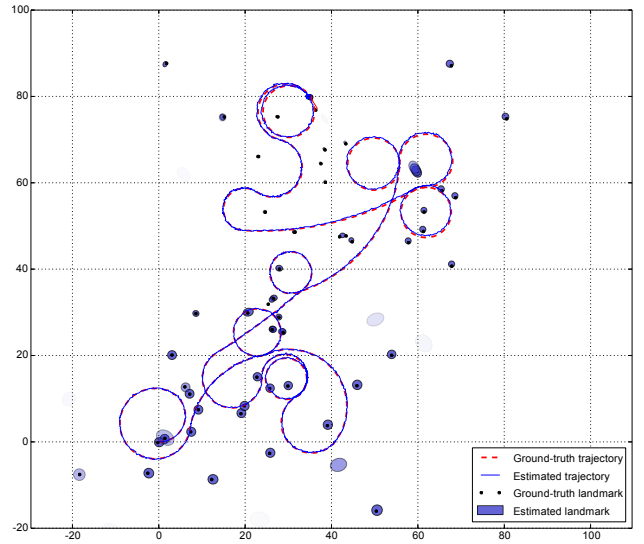


(b) FastSLAM

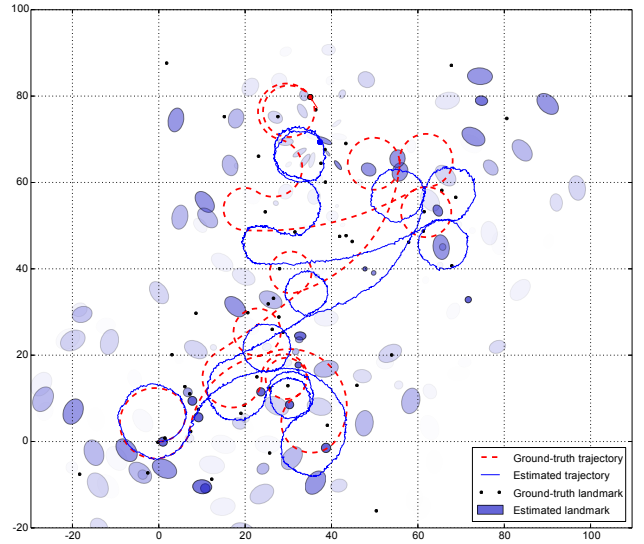
Fig. 2: The SLAM solution under the case 1 conditions ($P_D = 0.99, \kappa = 0.000001\text{m}^{-2}$).

was poor. Hence, the GPS trajectory will not be shown. The groundtruth map was made by manually identifying circular objects from scan-matched lidar scans from 17 static positions.

The results from processing the low clutter dataset is shown in Fig. 4, and those from the high clutter dataset is shown in Fig. 5. The groundtruth figure-eight path traversed by the robot can be seen in the satellite image underlays. As in the simulation results, RB-PHD-SLAM and FastSLAM performed similarly under the ideal conditions, while the FastSLAM estimate diverged under the non-ideal conditions. Note for the low-clutter case that the maps for RB-PHD-SLAM and FastSLAM are different. This is caused by the combination of not knowing the exact detection statistics for RB-PHD-SLAM, and non-zero clutter intensity for FastSLAM. Nevertheless, the resulting robot trajectories are similar for the low-clutter case.



(a) RB-PHD-SLAM

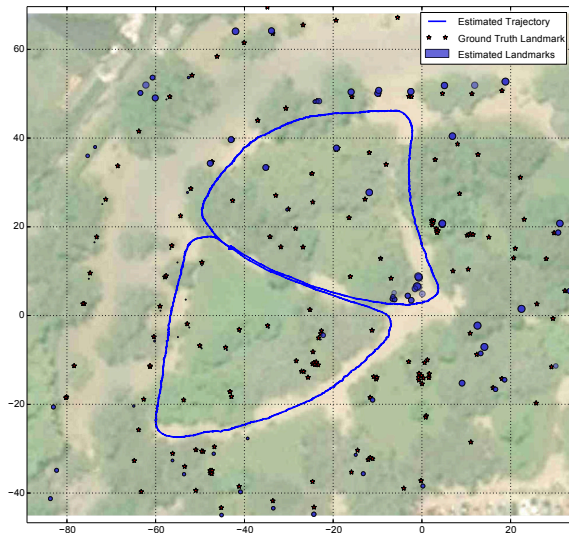


(b) FastSLAM

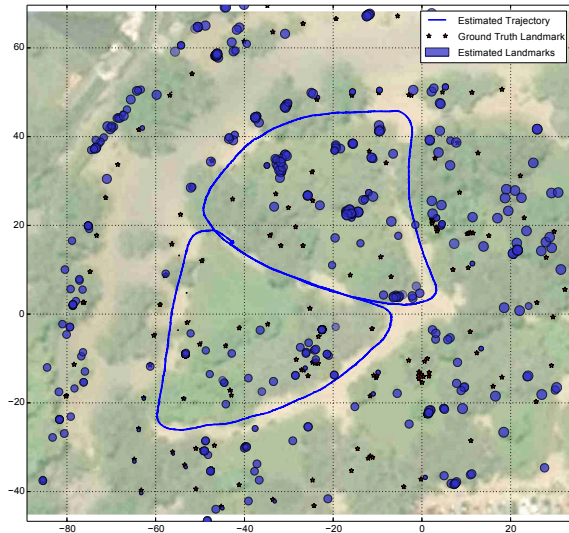
Fig. 3: The SLAM solution under the case 2 conditions ($P_D = 0.50, \kappa = 0.005000\text{m}^{-2}$).

V. CONCLUSION

RFS SLAM is an alternative to vector-based SLAM that allows the estimator to incorporate non-heuristic-based data association and detection statistics to estimate both the location and number of landmarks. A set of ideal detection conditions were define, under which the RFS Bayes estimator reduces to the random-vector form, and it was mathematically shown that RFS SLAM is a generalization of vector-based SLAM. Using the RFS-based RB-PHD SLAM and vector-based FastSLAM algorithms, simulations and real experiments were performed to validate the claim. With close-to-ideal detection conditions, both SLAM methods performed similarly as predicted. Under non-ideal conditions, the FastSLAM solution diverged due to the inherent ideal detection assumptions in vector-based approaches, while the generalized RFS-SLAM approach



(a) RB-PHD-SLAM



(b) FastSLAM

Fig. 4: SLAM solutions from the low-clutter dataset.

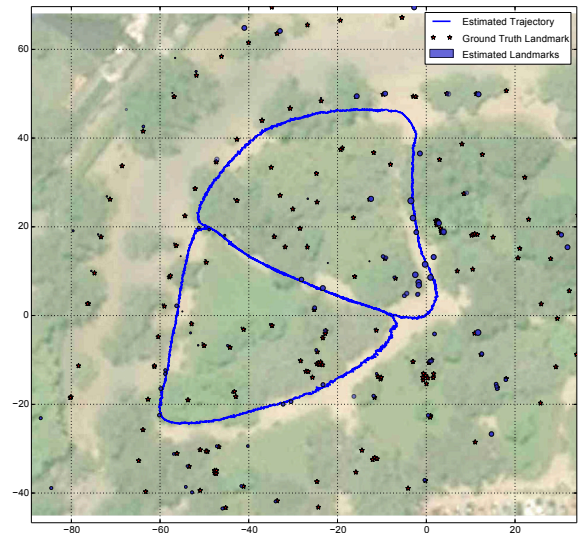
demonstrated a superior performance over a much wider range of detection and false alarm probabilities.

ACKNOWLEDGEMENTS

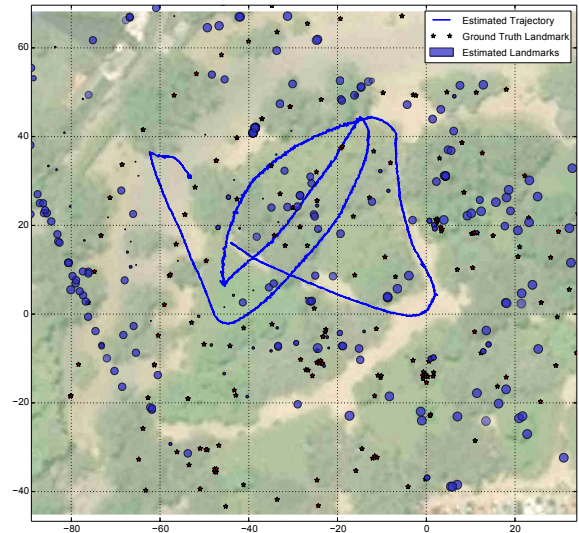
Conicyt - Fondecyt grant 1110579, Fondecyt Postdoctoral grant 3150066, and Clearpath Robotics.

REFERENCES

- [1] H. Durrant-Whyte and T. Bailey. Simultaneous localization and mapping: part I. *IEEE Robot. Autom. Mag.*, 13(2):99–110, 2006.
- [2] J. Mullane, B.-N. Vo, M. D. Adams, and B.-T. Vo. A random-finite-set approach to bayesian SLAM. *IEEE Trans. Robot.*, 27(2):268–282, 2011.
- [3] C. S. Lee, D. Clark, and J. Salvi. SLAM with dynamic targets via single-cluster PHD filtering. *IEEE J. Sel. Topics Signal Process.*, 7(3):543–552, 2013.
- [4] D. Moratuwage, D. Wang, A. Rao, N. Senarathne, and H. Wang. Rfs collaborative multivehicle slam: Slam in dynamic high-clutter environments. *IEEE Robot. Autom. Mag.*, 21(2):53–59, June 2014.
- [5] C. Lundquist, L. Hammarstrand, and F. Gustafsson. Road intensity based mapping using radar measurements with a probability hypothesis density filter. *IEEE Trans. Signal Process.*, 59(4):1397–1408, 2011.



(a) RB-PHD-SLAM



(b) FastSLAM

Fig. 5: SLAM solutions from the high-clutter dataset.

- [6] R. P. S. Mahler. *Statistical Multisource-Multitarget Information Fusion*, volume 685. Artech House Boston, 2007.
- [7] K. Y. K. Leung, F. Inostroza, and M. Adams. An improved weighting strategy for rao-blackwellized probability hypothesis density simultaneous localization and mapping. In *Proc. IEEE Int. Conf. Control, Automation, and Information Sciences*, 2013.
- [8] K. Y. K. Leung, F. Inostroza, and M. Adams. Evaluating set measurement likelihoods in random-finite-set slam. In *Proc. IEEE Int. Conf. Information Fusion*, Salamanca, Spain, 7 - 9 Jul 2014.
- [9] M. Montemerlo, S. Thrun, D. Koller, B. Wegbreit, et al. FastSLAM: A factored solution to the simultaneous localization and mapping problem. In *Proc. Nat. Conf. on Artificial Intelligence*, pages 593–598, 2002.
- [10] B.-N. Vo and W.-K. Ma. The Gaussian mixture probability hypothesis density filter. *IEEE Trans. Signal Process.*, 54(11):4091–4104, 2006.
- [11] S. Thrun, W. Burgard, and D. Fox. *Probabilistic robotics*, volume 1. MIT press Cambridge, 2005.
- [12] H. W. Kuhn. The hungarian method for the assignment problem. *Naval research logistics quarterly*, 2(1-2):83–97, 1955.
- [13] F. Inostroza, K. Y. K. Leung, and M. Adams. Set-based simultaneous localization and mapping using laser-range-based features. In *Proc. IEEE Int. Conf. Information Fusion*, Salamanca, Spain, 7 - 9 Jul 2014.